FULL PAPER

Homogeneous Photocatalytic H_2 Production using a Ru(II) Bathophenanthroline MLCT Photosensitizer

Rony S. Khnayzer,*[a] Babatunde S. Olaiya,[b],† Karim A. El Roz[c] and Felix N. Castellano*[c]

Abstract: The prototypical $Ru(bpy)_3^{2+}$ [bpy = 2,2'-bipyridine] photosensitizer has been previously demonstrated to be labile in aqueous photocatalytic solutions, especially in the presence of coordinating electron donors. Here, we describe an alternative Ru(II) molecular sensitizer, $Ru(dpp)_3^{2+}$ [dpp = 4,7-diphenyl-1,10-phenanthroline or bathophenanthroline] that is considerably more stable allowing enhanced photocatalysis metrics in conjunction with a cobalt glyoxime ($Co(dmgH)_2pyCl$) water reduction catalyst and N,N-dimethyl-p-toluidine (DMT) as sacrificial donor in 1:1 CH_3CN/H_2O. Photoluminescence studies revealed that DMT reductively quenches the excited state of $Ru(dpp)_3^{2+}$ with a bimolecular rate constant of $k_q = 4.9 \times 10^9\ M^{-1}\ s^{-1}$. The rate constant measured for electron transfer from the reduced sensitizer to the $Co(dmgH)_2(py)Cl$ was found to be near diffusion limits, $k_{Co} = 2.4 \times 10^9\ M^{-1}\ s^{-1}$. H_2 production photocatalysis independently monitored using a high-throughput photochemical reactor equipped with pressure transducers, gas chromatography, and mass spectrometer detection, illustrated that the composition yields high turnover numbers (TONs), approaching 10,000 (H_2/Ru) with respect to sensitizer while deuteration studies using D_2O confirmed that H_2 is primarily produced from protons derived from water in these systems.

Introduction

Hydrogen is a desirable high energy feedstock chemical whose oxidation leads to the formation of water and energy as product.[1] Hydrogen gas is currently being produced on industrial scales through steam reforming of natural gas. However, these current processes produce substantial amounts of greenhouse gases as by-products, and the respective cost of energy production is still several folds higher than those obtained from fossil fuels.[2] Therefore, alternative methods for producing hydrogen in the future must be engineered in order to provide a sustainable source of renewable energy to meet the growing global demand for chemical fuels. Inspired by examples in nature, efforts have been focused on developing biomimetic artificial photosynthetic schemes[3] capable of storing solar energy in the form of electricity or chemical bonds. Throughout the search for molecular systems for hydrogen production from water, researchers have commonly used the prototypical $Ru(bpy)_3^{2+}$ [bpy = 2,2'-bipyridine] and its derivatives as photosensitizers.[4] $Ru(bpy)_3^{2+}$ has been extensively studied for more than 50 years due to its attractive photophysical and electrochemical properties.[5] This sensitizer is commercially available, and possesses appropriate energetics to support both water oxidation and water reduction.[6] However, $Ru(bpy)_3^{2+}$ is known to be unstable due to ligand loss and photoanation.[7] This photochemistry has been shown to be thermally activated, since the dissociative ligand field metal centered triplet state ^{3}*MC is ~ 3600 cm^{-1} above the lowest triplet metal-to-ligand charge transfer excited state ^{3}*MLCT.[7b] Despite the intrinsic instability of this sensitizer in solution, especially in the presence of high concentration of potential ligands including H_2O and ascorbate electron donors, it is still widely utilized in photocatalysis.[8] In the midst of new advances in designing highly stable electrocatalytic water reduction catalysts composed of earth abundant materials,[9] the search for new photosensitizers with suitable high turnover parameters becomes obviated. Ir(III)[10] and Re(I)[3d, 11] molecules have demonstrated superior performance compared to $Ru(bpy)_3^{2+}$, but they generally suffer from small extinction coefficients in the visible region. In addition, Pt(II)[12] charge transfer complexes and organic triplet sensitizers[13] have been employed in photocatalysis and they commonly photobleach throughout extended photoactivation. These light harvesters have been incorporated into systems using numerous water reduction catalysts including various derivatives of cobalt glyoxime,[12a, 14] cobalt-dithiolenes,[15] biomimetic iron complexes,[16] nickel thiolates[17] and more recently a series of tetra and pentadentate-polypyridyl cobalt complexes[18]. Cobalt glyoximes have been used as water reduction catalysts given their low overpotential for hydrogen evolution and reasonable stability in aqueous solutions.[12a, 14a] However, $Co(dmgH)_2pyCl$ is known to undergo ligand dissociation and hydrogenation leading to the progressive loss of catalytic activity when using this family of molecules.[14] Commonly used sacrificial electron donors in homogeneous photocatalysis include ascorbic acid, triethylamine (TEA) and triethanolamine (TEOA); but one of the key setbacks to developing a system that produces hydrogen with high efficiency and stability is the lack of mechanistic insight that can be gleaned into the electron transfer reaction intermediates as these donors decompose into high energy reactive species. Dimethylaniline (DMA) has been used as an electron donor in conjunction with a supramolecular complex $[(bpy)_2Ru^{II}(dpp)_2Rh^{III}Cl_2](PF_6)_5$ (bpy = 2,2'-bipyridine and dpp = 2,3-bis(2-pyridyl)pyrazine).[19] However, DMA also decomposes into destructive products that prevent quantitative investigations into the catalytically important electron transfer processes. Structurally related N,N-dimethyl-*p*-toluidine (DMT) behaves distinctively different upon one electron oxidation, undergoing an electron transfer to form a DMT radical cation which proceeds through a series of reactions to form the stable N,N,N',N'-tetramethyl-α,α'-bi-*p*-toluidine dimer (TMBT).[20] This reaction product possesses an almost identical redox potential as DMT,[20] therefore, catalysis is not limited by the chemistry occurring with the sacrificial donor. Previous work from our group

[a] Dr. Rony S. Khnayzer
Department of Natural Sciences
Lebanese American University
Chouran, Beirut 1102-2801, Lebanon
E-mail: rony.khnayzer@lau.edu.lb
[b] Department of Chemistry
Bowling Green State University
Bowling Green, Ohio 43403, USA
† Current address: Eastman Chemical Company, 345 Beaver Creek Drive, Martins-ville, VA 24112.
[c] Prof. Felix N. Castellano
Department of Chemistry
North Carolina State University
2620 Yarbrough Drive, Raleigh, North Carolina, 27695, USA
E-mail: fncastel@ncsu.edu

Supporting information for this article is available on the WWW under http://dx.doi.org/10.1002/cplu.2014xxxxx."

has shown that DMT permits the use of time-resolved spectroscopy to illustrate the mechanism of hydrogen production in molecular photocatalysis experiments.[21] Alberto and co-workers were also able to extract useful kinetic parameters regarding rate constants of electron transfer from sensitizer to catalyst using infrared pump-probe experiments on a system which consisted of a rhenium carbonyl complex as photosensitizer and cobalt as water reduction catalyst.[18c, 22] Sutin and coworkers used laser flash photolysis to determine the formation of a key intermediate of cobalt formed during photocatalysis.[23] In addition, Gray and co-workers have used time resolved spectroscopy to monitor short lived species and determine electron self-exchange rate constants between various cobalt species during photocatalysis.[24] More recently, our laboratory employed transient-absorption spectroscopy to elucidate the intermediate and extract kinetics parameters of novel cobalt polypyridine catalysts in pure water.[25]

In the present work, $Ru(dpp)_3^{2+}$ [dpp = 4,7-diphenyl-1,10-phenanthroline = bathophenanthroline] is shown to display superior photostability and H_2 forming photocatalysis metrics with respect to $Ru(bpy)_3^{2+}$ using a cobalt glyoxime ($Co(dmgH)_2pyCl$) water reduction catalyst and DMT as the sacrificial electron donor in 1:1 CH_3CN/H_2O solvent mixtures. The multi-electron transfer steps eventually leading to H_2 formation were probed using photoluminescence and transient-absorption spectroscopy.

Results and Discussion

The homogenous system investigated here consists of the ruthenium(II) *tris*-bathophenanthroline, $Ru(dpp)_3^{2+}$, as photosensitizer, $Co(dmgH)_2(py)Cl$ as the water reduction catalyst and DMT as the sacrificial electron donor, whose structures are presented in Figure 1.

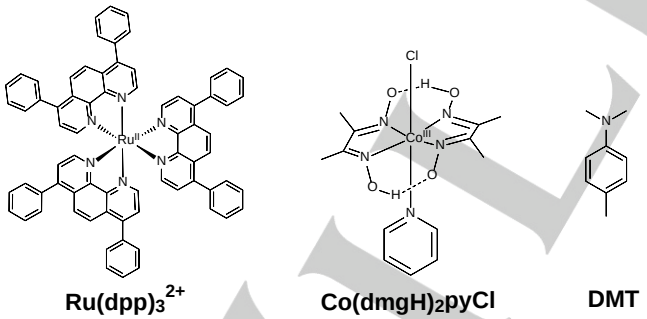

Figure 1. Structures of $Ru(dpp)_3^{2+}$, $Co(dmgH)_2pyCl$ and DMT.

$Ru(dpp)_3^{2+}$ has a higher extinction coefficient (ε ~ 27,000 M^{-1} cm^{-1}) and is slightly red-shifted with respect to the prototypical $Ru(bpy)_3^{2+}$ (ε ~ 14,000 M^{-1} cm^{-1}) in its visible MLCT absorption bands enabling more efficient harvesting of sunlight energy.[26] In addition, the hydrophobic phenanthroline ligand framework was previously found to be more robust than bipyridine when coordinated to various metal centers.[27] $Ru(dpp)_3^{2+}$ has a notably long excited state lifetime (τ = 5.86 μs) in 1:1 CH_3CN/H_2O facilitating bimolecular electron transfer reactions featuring diffusion limited kinetics.

Samples containing 3.6 x 10^{-5} M of $Ru(dpp)_3^{2+}$, 6.2 x 10^{-4} M of $Co(dmgH)_2(py)Cl$, and 7 x 10^{-2} M of DMT in 10 mL solution of 1:1 CH_3CN/H_2O were irradiated with 540 mW excitation at 452 ± 10 nm while varying the pH of each sample. Figure S1 shows that the optimum pH for this system lies between 6.0-6.5. The ability to operate at or near neutral pH is very important for the fundamental understanding of systems that are able to evolve hydrogen at physiological pH.[25] Under acidic conditions, protonation of the amino group on DMT is favorable, resulting in suppressed donation of electrons to the photosensitizer, whereas in basic buffer media, the cobalt catalyst would be limited by proton accessibility to the metal center leading to low photocatalytic yields.[13a] Based on this rationale, DMT is a promising candidate, energetically and kinetically, to act as a sacrificial electron donor at moderate to neutral pH suitable for catalysis.[21]

Importantly, when the $Ru(dpp)_3^{2+}$ photosensitizer was directly compared to $Ru(bpy)_3^{2+}$ in combinatorial photoreactions under identical conditions (7.2 × 10^{-5} M of Ru(II) photosensitizer, 6.2 × 10^{-4} M of $Co(dmgH)_2pyCl$, and 7 × 10^{-2} M of DMT), the former had significantly higher stability in 1:1 $CH_3CN:H_2O$ leading a higher fidelity for the associated catalytic composition, Figure 2.

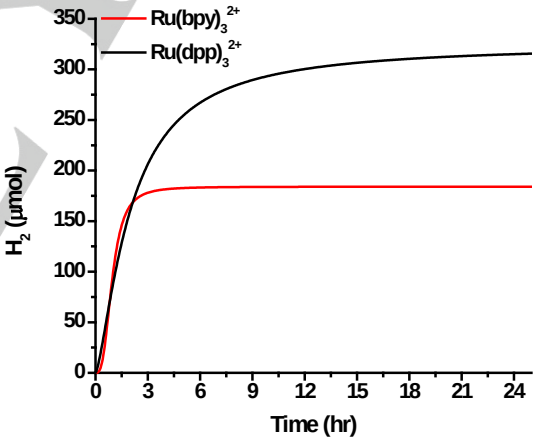

Figure 2. Comparison between the photocatalytic hydrogen production of $Ru(dpp)_3^{2+}$ and $Ru(bpy)_3^{2+}$ at the same concentration of 7.2 × 10^{-5} M Ru(II), 6.2 × 10^{-4} M $Co(dmgH)_2pyCl$, and 7 × 10^{-2} M DMT in 1:1 $CH_3CN:H_2O$.

Similarly, the initial rates of hydrogen production were comparable but the fidelity of the system deteriorated in the latter case as evidenced by fewer moles of hydrogen accumulated in the headspace of the photoreactor, Figure 2. The superior stability of the $Ru(dpp)_3^{2+}$ / $Co(dmgH)_2pyCl$ / DMT system over $Ru(bpy)_3^{2+}$/ $Co(dmgH)_2pyCl$ / DMT can be attributed to rigidity of $Ru(dpp)_3^{2+}$ that is less prone to ligand loss/substitution.[7a, 7d, 7f] These results imply that the bathophenanthroline framework likely provides better stability to the photosensitizer than its bipyridyl counterpart, while still providing efficient electron transfer and hydrogen

evolution dynamics. To verify that photocatalysis was not brought about by in-situ formation of colloidal cobalt nanoparticles and that the current system was strictly homogeneous, a mercury poisoning experiment was conducted under constant shaking, Figure S2.[28] There was no significant change in the rate or total amount of H_2 evolved in the presence or absence of mercury that likely indicates no formation of colloidal catalytic material(s), Figure S2. The turnover number (TON) vs. [$Ru(dpp)_3^{2+}$] increased with decreasing concentration of $Ru(dpp)_3^{2+}$ achieving ~ 10,000 (H_2/Ru) when using 1.44 x 10^{-6} M of $Ru(dpp)_3^{2+}$, 2.5 x 10^{-3} M of $Co(dmgH)_2pyCl$ and 7 x 10^{-2} M of DMT after 30 h of irradiation, Figure S3. This value is amongst the highest TON vs. sensitizer for any homogeneous transition metal based photosensitizer system in concert with a molecular cobalt catalyst in mixed co-solvent to date, Figure S3.[29]

Control experiments were carried out and no hydrogen was evolved in the absence of any of the three components in the system. The stability of the sensitizer was tested through regeneration experiments. At intervals of 16 hours after catalysis had ceased, a fresh equivalent amount of $Co(dmgH)_2pyCl$ was added to the sample and the pH was re-adjusted to 6.0, Figure 3.

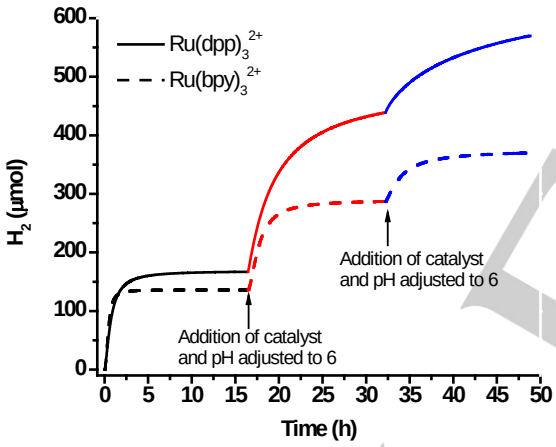

Figure 3. Hydrogen evolution regeneration following the addition of an equivalent of $Co(dmgH)_2pyCl$ and pH adjustment to 6.0 to samples containing 1.44 x 10^{-4} M $Ru(dpp)_3^{2+}$ (bold lines) or 1.44 x 10^{-4} M $Ru(bpy)_3^{2+}$ (dashed lines), 3.7 x 10^{-4} M $Co(dmgH)_2pyCl$ and 7 x 10^{-2} M of DMT in 1:1 CH_3CN:H_2O at intervals of 16 h following photolysis.

It was also observed that photocatalysis completely recovered after the addition of $Co(dmgH)_2pyCl$ and the initial rate became slower only during the third cycle due to the slight decomposition of the photosensitizers and DMT during the course of the photocatalytic experiments as well as possible formation of side-products that can influence electron transfer dynamics, Figure S4a.[11a] After each catalytic cycle, the measured pH increased by 0.2-0.5 pH unit. The protons consumed during hydrogen evolution can be partially replenished following the decomposition of the electron donor in solution as is the case for other electron donors.[25] As stated earlier, cobalt glyoximes are known to readily undergo ligand loss and possible hydrogenation which might lead to bi-product build-up in solution and loss of catalytic activity.[14] Eisenberg and coworkers studied the mechanism and bi-products of cobalt glyoxime decomposition under photocatalytic conditions.[14b] UV-Vis absorption spectra measured for the various catalytic compositions containing $Ru(dpp)_3^{2+}$ did not exhibit any significant changes in the MLCT absorption band even after three full cycles of photocatalysis, Figure S4a. In the case of $Ru(bpy)_3^{2+}$, the MLCT absorption band was, to a less extent, maintained throughout photocatalysis, Figure S4b. These data suggest that the improved performance and regeneration of catalysis observed here is a result of using DMT as electron donor which imparted stability onto both sensitizers. However, the higher number of moles of hydrogen generated and the decrease of MLCT absorption band alteration in the $Ru(dpp)_3^{2+}$ / $Co(dmgH)_2pyCl$ / DMT versus $Ru(bpy)_3^{2+}$/ $Co(dmgH)_2pyCl$ / DMT system suggests that $Ru(dpp)_3^{2+}$ outperforms $Ru(bpy)_3^{2+}$ in side-by-side comparison of photocatalytic metrics.

The quantum yield of hydrogen generation for the $Ru(dpp)_3^{2+}$ / $Co(dmgH)_2pyCl$ / DMT system was found to be 6.5 ± 0.4 % which is comparable to recently reported value utilizing robust cobalt polypyridine molecular catalysts and $Ru(bpy)_3^{2+}$ photosensitizer in pure water.[25]

To verify that hydrogen generation results primarily from the reduction of water-based protons and not organic substances present in solution, deuteration experiments were performed using D_2O in place of H_2O. The source of protons for hydrogen evolution in these compositions was elucidated using mass spectrometry (MS) analysis. In these experiments, water was replaced by D_2O and HCl by DCl while all other constituents remained the same. This furnished a solvent composition $D_2O/CH_3CN/DCl$ containing $Ru(dpp)_3^{2+}$, $Co(dmgH)_2pyCl$ and DMT. The sample was irradiated with visible light and the headspace sample was analyzed with a residual gas analyzer MS after equilibration to atmospheric pressure, Figure 4. The background of hydrogen was collected from the headspace of a solution containing pure H_2O/CH_3CN/DMT (without the addition of photosensitizer, catalyst or electron donor) under 1 atm of Ar, Figure 4. After photolysis, the sample with $D_2O/CH_3CN/DCl$ as solvent showed > 90% deuterium incorporated in the gaseous product with D_2 being the major product and HD a minor product suggesting that the main source of hydrogen are protons in water. The small amount of H_2 present in the sample was mainly attributed to mass spectrometer outgassing and not from the photocatalytic reaction since a comparable amount was present in the background.

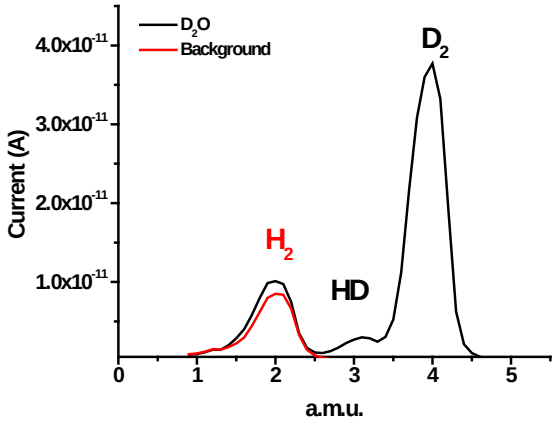

Figure 4. MS analysis of the headspace of a sample containing 3.6 x10^{-5} M of $Ru(dpp)_3^{2+}$, 6.2 x 10^{-4} M of $Co(dmgH)_2pyCl$ and 7 x 10^{-2} M of DMT in 1:1 ratio of D_2O/CH_3CN acquired after the cease of photocatalysis (black line). The pH was adjusted to 6.0 using DCl. The background represents the headspace mass spectrometry analysis of a solution containing H_2O/CH_3CN/DMT under 1 atm of Ar (red line).

Photoluminescence quenching studies were carried out on samples containing $Ru(dpp)_3^{2+}$ with varying concentration of $Co(dmgH)_2pyCl$ or DMT in a degassed solution of 1:1 CH_3CN/H_2O. Stern-Volmer analysis revealed that both reductive and oxidative quenching pathways occur in this system. Reductive and oxidative quenching rate constants of 4.9 × 10^9 M^{-1} s^{-1} and 3.6 × 10^9 M^{-1} s^{-1} were obtained respectively, Figures S5 and S6. The excited state lifetime of $Ru(dpp)_3^{2+}$ was found to be 5.86 µs in deaerated 1:1 ACN:H_2O, Figure S7. Given the large excess of DMT used with respect to the cobalt catalyst under catalytic conditions, the reductive quenching mechanism of $[Ru(dpp)_3^{2+}]$***** is likely to be predominant here. Note that multiple electrons have to be delivered to the cobalt catalyst in order to produce hydrogen in these instances.[24, 30] In order to investigate the various routes of electron transfer in this system, both transient absorption experiments were carried out on samples containing $Ru(dpp)_3^{2+}$ alone **(a)** ; $Ru(dpp)_3^{2+}$ and DMT **(b)**; $Ru(dpp)_3^{2+}$**,** $Co(dmgH)_2pyCl$ and DMT **(c)** respectively, Figure 5. Upon excitation of a sample containing $Ru(dpp)_3^{2+}$ in 1:1 mixture of CH_3CN:H_2O with λ_{exc} = 460 nm (~ 4.5 mJ/pulse), the difference spectra were obtained with typical excited state absorption bands of $Ru(dpp)_3^{2+}$ centered around 350 nm and 550 nm and a ground state bleach centered around 450 nm. Kinetic decay traces were measured at different peak wavelengths and was found to be mono-exponential with τ ~ 5.6 µs corresponding to the excited state lifetime of $Ru(dpp)_3^{2+}$, Figure 5a inset.

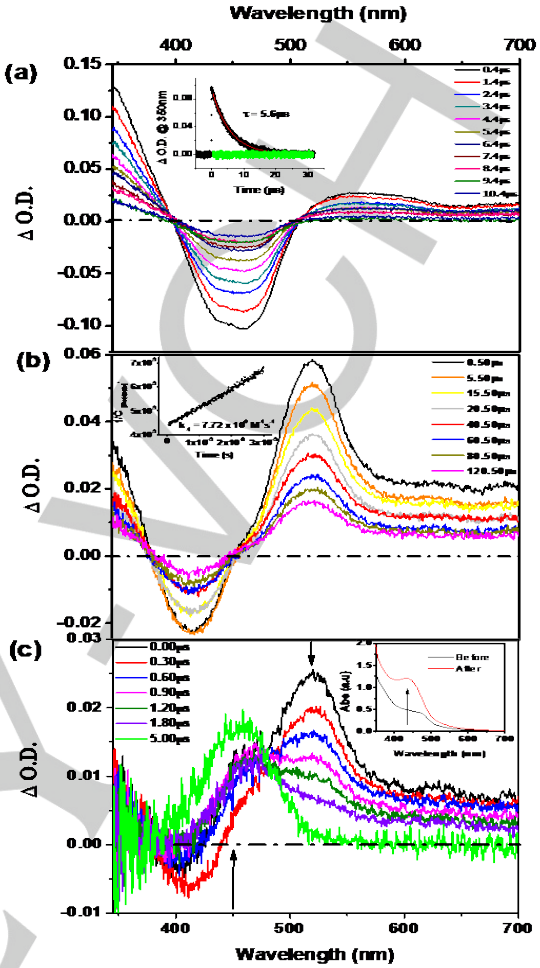

Figure 5. **(a)** Transient absorption difference spectra of $Ru(dpp)_3^{2+}$ (8.2 x 10^{-6} M) under different conditions. Inset: Kinetic decay trace of sample at 525 nm. The green line represents the residuals of the fit. **(b)** Transient absorption of $Ru(dpp)_3^{2+}$ in the presence of 7 x 10^{-2} M of DMT. Inset shows kinetic trace of the sample at 525 nm plotted as 1/[$Ru(dpp)_3^{+}$] vs. time. **(c)** Transient absorption spectra of $Ru(dpp)_3^{2+}$, $Co(dmgH)_2pyCl$ (3 x 10^{-4} M) and DMT (7 x 10^{-2} M). Inset shows the steady-state UV-Vis absorption spectrum of the sample before and after laser flash photolysis. All spectra were acquired from 3 ml solution of 1:1 mixture of CH_3CN/H_2O with λ_{exc} = 460nm (~4.5 mJ/pulse).

The transient difference spectrum of a separate sample containing the same concentration of $Ru(dpp)_3^{2+}$ and 7 x 10^{-2} M of DMT was also taken. It was observed that upon excitation a new absorption feature appears centered at 525 nm, Figure 5b. This absorption band was assigned, based on spectroelectrochemistry, to the $Ru(dpp)_3^{+}$ radical anion, which is produced following reductive electron transfer from DMT to $[Ru(dpp)_3^{2+}]$***,** Figure S8. The ground state absorption spectrum of the sample before and after the transient absorption study did not show any changes indicating complete reversibility of the electron transfer processes on long time scales. In addition, the absorption feature at 525 nm decayed back to zero indicating the

recombination of $Ru(dpp)_3^+$ with $DMT^{\cdot+}$, Figure 5b. In the absence of any cobalt catalyst, the kinetic decay traces at 525 nm were adequately fit with second order equal concentration kinetics to obtain the back recombination rate constant between the $DMT^{\cdot+}$ and $Ru(dpp)_3^+$, $k_b = 7.7 \times 10^9\ M^{-1}\ s^{-1}$, Figure 5b inset. The cage escape yield for the $Ru(dpp)_3^+$/ $DMT^{\cdot+}$ pair was found to be rather large, $\Phi_{cage} \sim 75\ \%$, so most of the absorbed photons result in separated electron transfer products that are available for subsequent reactions. Samples containing the same concentration of $Ru(dpp)_3^{2+}$, DMT in addition to 3×10^{-4} M of $Co(dmgH)_2pyCl$ was also prepared and degassed. The transient difference spectra collected showed the growth of a band at 450 nm and the decay of the 525 nm band within a 5 µs time window, Figure 5c. This is rationalized by fast electron transfer from $Ru(dpp)_3^+$ to $Co(dmgH)_2pyCl$ yielding the ground state of $Ru(dpp)_3^{2+}$ and the corresponding Co^{2+} species. The ground state absorption spectrum taken after laser flash photolysis experiments showed the growth of the band at 450 nm which was attributed to the buildup of Co^{2+} in the system which eventually enters the hydrogen evolution cycle once it reaches a critical concentration, Figure 5c inset.

The rate of electron transfer from $Ru(dpp)_3^+$ to $Co(dmgH)_2pyCl$ was determined using kinetic decay traces at 525 nm of samples containing different concentrations of $Co(dmgH)_2pyCl$. The transients were collected and plot of the inverse lifetime of $Ru(dpp)_3^+$ radical anion ($1/\tau_{Ru(dpp)_3^+} = k_{obs}$ where k_{obs} is the observed rate constant) vs. $[Co(dmgH)_2pyCl]$ yielded a rate constant for the electron transfer from $Ru(dpp)_3^+$ to the cobalt catalyst of $k_{Co} = 2.4 \times 10^9\ M^{-1}\ s^{-1}$, Figure 6 inset. Note that the Co^{2+} absorption tail slightly overlaps with the absorption band of $Ru(dpp)_3^+$ at 525 nm rendering the decays in Figure 6 biexponential in nature. k_{Co} was calculated only from the main component which is short lived and attributed to the decay of $Ru(dpp)_3^+$.

Photoluminescence and transient-absorption spectroscopy yielded valuable mechanistic insights into the photocatalytic hydrogen production steps. Under visible light irradiation, the excited state of the photosensitizer ($[Ru(dpp)_3^{2+}]^*$) undergoes predominantly reductive quenching by DMT to yield highly energetic radicals ($Ru(dpp)_3^+$). These species subsequently reduce $Co(dmgH)_2(py)Cl$ in multiple electron transfer steps, Scheme 1. The first two electron-transfer steps from the electron donor to the photosensitizer and then to the catalyst occur with rate constants on the order of $10^9\ M^{-1}s^{-1}$. A critical concentration of reduced cobalt catalyst has to be generated before entering the hydrogen production cycle. These results are consistent with steady-state experiments on similar cobalt glyoxime molecular catalysts whereby the reduced state of the catalyst accumulates in solution and can be detected via absorption experiments as a function of irradiation.[14a]

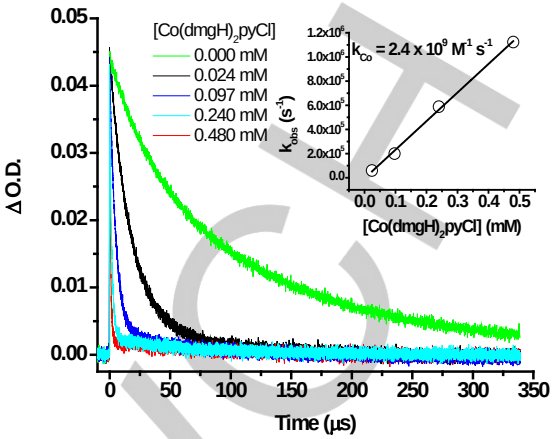

Figure 6. Kinetic decay trace of a sample at 525 nm with λ_{exc} = 460 nm (~ 5.8 mJ/pulse) containing $Ru(dpp)_3^{2+}$ (8.2×10^{-6} M), DMT (7×10^{-2} M) and a varied concentration of $Co(dmgH)_2pyCl$ in 1:1 mixture of CH_3CN and H_2O. Inset shows plot of k_{obs} vs. $[Co(dmgH)_2pyCl]$.

Scheme 2 illustrates the energy level diagram extracted from electrochemical measurements (see Figure S10-S12 and Table S1) comparing the relevant redox potentials of species used in this work. The DMT oxidation occurs slightly more positive than excited state reduction potential sensitizers (termed *Red in scheme 2) paving the way for possible reductive quenching of the excited state of both $Ru(bpy)_3^{2+}$ and $Ru(dpp)_3^{2+}$ by DMT electron donor. Note that the excited state oxidation potential (termed *Ox in scheme 2) is more negative than Co^{3+}/Co^{2+} reduction potential, supporting the feasibility of oxidative quenching pathway. However, as previously mentioned, the reductive quenching mechanism is predominating since DMT is present in 1-2 orders of magnitude higher than the cobalt catalyst. Added to that, the reduction of Co^{2+}/Co^+ is not thermodynamically accessible from the excited state of Ru(II) photosensitizer. It is noticeable that the reduced Ru(II) photosensitizer (termed L^- in scheme 2) that results from the reductive quenching pathway is energetically poised for the reduction of Co^{3+} to Co^{2+} and Co^{2+} to Co^{+1}. The latter is thermodynamically well positioned for catalytic proton reduction and is believed to form cobalt hydride, an important intermediate in the hydrogen evolution mechanism.[14a] The energy diagram in scheme 2 strongly supports the mechanism of hydrogen evolution proposed in Scheme 1.

Scheme 1. Schematic representation of the multi-step electron transfer mechanism and kinetic parameters. Dashed arrows depict steps that were not directly observed in transient absorption spectroscopy. Note that two electrons must be delivered from $[Ru(dpp)_3]^+$ to form one H_2 product. The Co^{2+} reduction to Co^+ can occur either via the disproportionation reaction of two Co^{2+} or the direct reduction of Co^{2+} by $[Ru(dpp)_3]^+$.

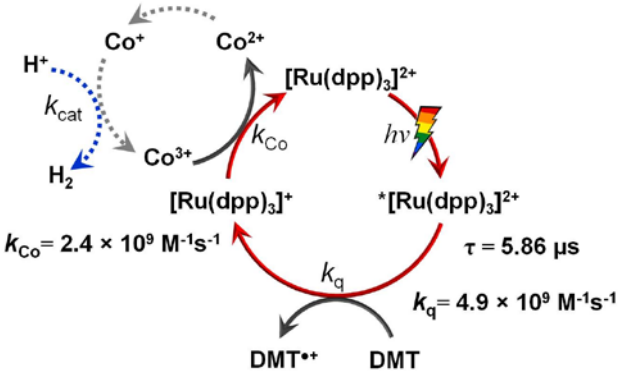

Scheme 2. Energy diagram depicting the oxidation/reduction potentials of the relevant species present in the catalytic compositions investigated in this work.

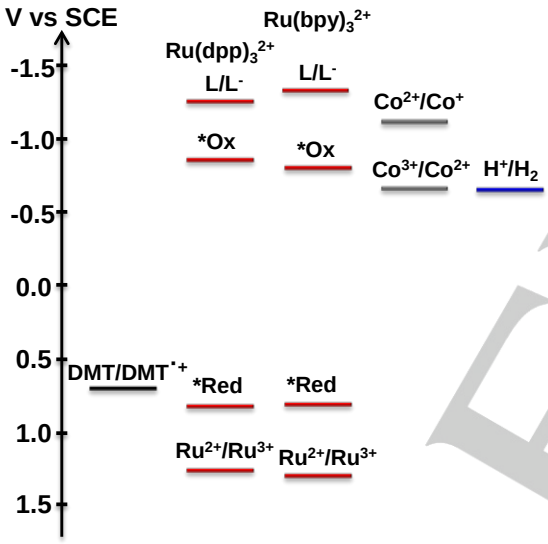

Conclusions

A new homogeneous photocatalytic proton reduction system consisting of $Ru(dpp)_3^{2+}$ as photosensitizer, $Co(dmgH)_2pyCl$ as catalyst, and DMT as sacrificial electron donor has been investigated. The photosensitizer significantly outperformed $Ru(bpy)_3^{2+}$ in side-by-side comparison photocatalytic longevity. The addition of fresh equivalent amount of $Co(dmgH)_2pyCl$ after the cease of hydrogen production has regenerated catalysis illustrating the robustness of the photosensitizer in the catalytic composition. The mechanism of hydrogen production was investigated by flash photolysis. The bimolecular reductive quenching rate constant of $Ru(dpp)_3^{2+}$ by DMT was $k_q = 4.9 \times 10^9$ M^{-1} s^{-1} and the rate of electron transfer from the $[Ru(dpp)_3]^+$ to $Co(dmgH)_2pyCl$ was found to be $k_{Co} = 2.4 \times 10^9$ M^{-1} s^{-1}. Deuteration studies showed that the source of hydrogen is likely protons from water when the system operated in 1:1 H_2O:ACN. DMT likely forms stable dimeric product[20] after oxidation, avoiding the production of highly reactive radical intermediates which is usually the case in tertiary amines and leading to the enhanced stability of the photosensitizer. A hydrophilic version of $Ru(dpp)_3^{2+}$ photosensitizers is much needed to replace $Ru(bpy)_3^{2+}$ in testing recently conceived molecular catalysts that are highly stable and earth-abundant. Water compatibility and tuning of the photophysical properties can be readily done by ligand alterations. The combined data in this manuscript represents important advancement towards the design of molecular photosensitizers that can operate in aqueous media.

Experimental Section

Materials. Tris(2,2'-bipyridyl) dichlororuthenium(II) hexahydrate ($Ru(bpy)_3Cl_2.6H_2O$), Cobalt(II) chloride hexahydrate ($CoCl_2.6H_2O$), N,N-Dimethyl-p-toluidine (DMT), tetrabutylammonium bromide (TBABr), dimethylglyoxime (dmgH), pyridine, tetrabutylammonium hexafluorophosphate ($TBAPF_6$), and ammonium hexafluorophosphate (NH_4PF_6) were purchased from Aldrich and used without further purification. $[Ru(dpp)_3]Cl_2$ was purchased from GFS chemicals and used without further purification. Water was deionized using a Barnstead nanopure system (~ 18 MΩ-cm). D_2O and DCl were purchased from Cambridge Isotope.

Synthesis of $[Ru(dpp)_3](PF_6)_2$. $[Ru(dpp)_3]Cl_2$ was converted to the hexafluorophosphate (PF_6^-) salt by adding an excess of ammonium hexafluorophosphate in water. Elemental analysis calcd (%) for C72H48F12N6P2Ru (1388.2): C 62.30, H 3.49, N 6.05; found: C 62.00, H 3.35, N 6.22.

Synthesis of $Co(dmgH)_2pyCl$. $Co(dmgH)_2pyCl$ was synthesized using an already published procedure.[31] Elemental analysis calcd (%) for C13H19ClCoN5O4 (403.71): C 38.68, H 4.74, N 17.35; found: C 38.87, H 4.64, N 17.53.

Hydrogen Generation Studies.[32] 10 mL samples of varying compositions were prepared in 40 mL air-tight EPA vial. All pH values reported in this work were measured using a pH meter (Mettler Toledo). A high throughput system equipped with 452 nm LED's was used as an excitation source. The temperature was fixed at 20 °C using a circulating water chiller. The headspace vials were degased before irradiation using a series of pressurizing cycles of vacuum/Argon followed by equilibrating to 1 atm allowing the vials to be under inert atmospheric pressure. The H_2 evolved was monitored in real time by the change in pressure (p51 pressure sensors, SSI technologies) and quantified after the completion of photocatalysis by sampling into a Shimadzu GC-8A equipped with a 5 Å molecular sieve column and thermal conductivity detector operated with ultra-high purity Ar carrier gas. In addition, the headspace which was pressurized by H_2 buildup during the course of photocatalysis, was equilibrated to atmospheric pressure and the percent of H_2 relative to Ar was analyzed by MS gas analyzer (UGA-H_2, SRS). GC and MS data were calibrated against a certified Ar/H_2 standard (Praxair). Quantitative results of hydrogen were typically averaged and the processed pressure data were normalized to the final amounts of hydrogen measured. For deuterated studies, the MS was used to sample the headspace to selectively quantify the percent of D_2, HD and H_2 that was produced during photocatalysis. The pH values reported here are directly measured by a pH-meter as previously detailed.[21] In the regeneration experiments, the pH increases by 0.2-0.5 pH unit after each cycle of photocatalysis and was adjusted using an aqueous solution of HCl to its original value.

Electrochemical Studies. Cyclic voltammetry and differential pulse voltammetry were carried out using a BAS potentiostat in an air tight cell under steady flow of argon with Pt or glassy carbon electrode as working, Pt wire as the counter electrode, Ag wire as reference and ferrocene was used as an internal standard. All potentials were then referenced vs. SCE. All electrochemical measurements were performed in anhydrous CH_3CN as solvent and 0.1 M tetrabutylammonium hexafluorophosphate as the supporting electrolyte.

Steady State Measurement. Absorption spectra were acquired using a Cary 50 or an Agilent 8453 diode array spectrophotometer. Static emission spectra were collected using a FL/FS920 spectrofluorimeter (Edinburgh Instruments) equipped with a 450 W Xe arc lamp and a Peltier cooled, red sensitive PMT (R2658P, Hamamatsu). All emission spectra were corrected for detector response. For each measurement, optically dilute (OD = 0.1-0.2) solutions were excited into the lowest energy absorption band and solutions were degassed by purging with a stream of Ar gas for a minimum of 30 minutes and the head space of the solutions were maintained under positive Ar pressure during data acquisition.

Dynamic Spectroscopic Measurements. Time-resolved photoluminescence and transient absorption data were collected with an LP920 laser flash photolysis system from Edinburgh Instruments. The excitation pump source was the Vibrant LD 355 II Nd:YAG/OPO system (OPOTEK). Data acquisition was controlled by the LP920 software program (Edinburgh Instruments). Samples were prepared with an optical density of 0.1 - 0.2 at the excitation wavelength for emission measurements and 0.3-0.5 at the excitation wavelength for transient absorption measurements. These samples were degassed identically as stated above. Kinetic traces were collected with a PMT (R928 Hamamatsu) and transient absorption difference spectra were collected using an iStar ICCD camera (Andor Technology). The associated kinetic traces were modeled using Origin 8.1. All rate constants and lifetime measurements were sensitive to the presence of oxygen and were acquired after thorough argon sparging. All measurements were repeated at least twice with <10% variation.

Spectroelectrochemistry (SEC). Spectroelectrochemistry experiments were executed in the glovebox in anhydrous CH_3CN. These measurements were performed using controlled-potential electrolysis (BAS potentiostat) at potentials 50-100 mV more negative than the reduction potential of the corresponding ruthenium compound. The change in absorption due to the reduction of the compound was monitored by the ocean optic spectrometer ocean optic spectrometer (HR2000+) for UV−visible experiments equipped with both deuterium and halogen light sources (DT-MINI-2-GS, Ocean Optics) which are coupled to fibre optic cords.

Cage escape calculation. The cage escape yield (Φ_{CE}) was calculated from transient absorption kinetic decay analysis using $Ru(bpy)_3^{2+}$ in water as actinometer according to the following equation:[33]

$$\Phi_{CE} = \frac{\Delta A_{sample} / \Delta\epsilon_{sample} \times (1 - 10^{-A_{actinometer}})}{\Delta A_{actinometer} / \Delta\epsilon_{actinometer} \times (1 - 10^{-A_{sample}}) \times fraction\ quenched}$$

Where ΔA_{sample} is the maximum of the decay of the radical anion, $\Delta\epsilon_{sample}$ was estimated from spectroelectrochemical measurement of the extinction coefficient at a particular wavelength, $\Delta A_{actinometer}$ is the maximum transient observed for the $Ru(bpy)_3^{2+}$ actinometer under identical excitation conditions, $\Delta\epsilon_{actinometer}$ ~ 22,000 $M^{-1}cm^{-1}$ as previously reported[33]. Both sample and actinometer had absorbance ~ 0.35, and the fraction quenched was calculated by extrapolation from the Stern-Volmer constant.

Acknowledgements

RSK acknowledges fund from the School Research and Development Council at LAU (SRDC-t2014-02) and the Lebanese National Council for Scientific Research (Ref: 05-06-14)

Keywords: Ruthenium • hydrogen • photocatalysis • time-resolved spectroscopy • electron transfer

[1] a) A. F. Heyduk, D. G. Nocera, *Science* **2001**, *293*, 1639-1641; b) M. Chanon, Ed., *Homogeneous Photocatalysis*, John Wiley & Sons, Chichester, UK, **1997**; c) A. Harriman, M. A. West, Eds., *Photogeneration of Hydrogen*, Academic Press, London, **1982**.

[2] A. J. Esswein, D. G. Nocera, *Chem. Rev.* **2007**, *107*, 4022-4047.

[3] a) W. J. Youngblood, S.-H. A. Lee, Y. Kobayashi, E. A. Hernandez-Pagan, P. G. Hoertz, T. A. Moore, A. L. Moore, D. Gust, T. E. Mallouk, *J. Am. Chem. Soc.* **2009**, *131*, 926-927; b) M. Gratzel, *Nature* **2001**, *414*, 338-344; c) L. L. Tinker, N. D. McDaniel, S. Bernhard, *J. Mater. Chem.* **2009**, *19*, 3328-3337; d) B. Probst, M. Guttentag, A. Rodenberg, P. Hamm, R. Alberto, *Inorg. Chem.* **2011**, *50*, 3404-3412; e) A. Fihri, V. Artero, A. Pereira, M. Fontecave, *Dalton Trans.* **2008**, *0*, 5567-5569; f) D. Gust, T. A. Moore, A. L. Moore, *Acc. Chem. Res.* **2009**, *42*, 1890-1898.

[4] a) K. Kalyanasundaram, J. Kiwi, M. Grätzel, *Helv. Chim. Acta* **1978**, *61*, 2720-2730; b) C. V. Krishnan, N. Sutin, *J. Am. Chem. Soc.* **1981**, *103*, 2141-2142; c) J. Kiwi, M. Gratzel, *Nature* **1979**, *281*, 657-658; d) J. M. Lehn, J. P. Sauvage, *Nouv. J. Chim.* **1977**, *1*, 449; e) G. M. Brown, B. S. Brunschwig, C. Creutz, J. F. Endicott, N. Sutin, *J. Am. Chem. Soc.* **1979**, *101*, 1298-1300; f) M. Kirch, J.-M. Lehn, J.-P. Sauvage, *Helv. Chim. Acta* **1979**, *62*, 1345-1384; g) S. F. Chan, M. Chou, C. Creutz, T. Matsubara, N. Sutin, *J. Am. Chem. Soc.* **1981**, *103*, 369-379.

[5] a) K. Kalyanasundaram, *Coord. Chem. Rev.* **1982**, *46*, 159-244; b) A. Juris, V. Balzani, F. Barigelletti, S. Campagna, P. Belser, A. von Zelewsky, *Coord. Chem. Rev.* **1988**, *84*, 85-277; c) E. Amouyal, *Sol. Energy Mater. Sol. Cells* **1995**, *38*, 249-276; d) N. Sutin, C. Creutz, in *Inorganic and Organometallic Photochemistry, Vol. 168*, American Chemical Society, **1978**, pp. 1-27.

[6] C. R. Bock, J. A. Connor, A. R. Gutierrez, T. J. Meyer, D. G. Whitten, B. P. Sullivan, J. K. Nagle, *J. Am. Chem. Soc.* **1979**, *101*, 4815-4824.

[7] a) J. Van Houten, R. J. Watts, *Inorg. Chem.* **1978**, *17*, 3381-3385; b) J. Van Houten, R. J. Watts, *J. Am. Chem. Soc.* **1976**, *98*, 4853-4858; c) J. Van Houten, R. J. Watts, *J. Am. Chem. Soc.* **1975**, *97*, 3843-3844; d) L. J. Henderson Jr, M. Ollino, V. K. Gupta, G. R. Newkome, W. R. Cherry, *J. Photochem.* **1985**, *31*, 199-210; e) G. H. Allen, R. P. White, D. P. Rillema, T. J. Meyer, *J. Am. Chem. Soc.* **1984**, *106*, 2613-2620; f) T. K. Foreman, J. B. S. Bonilha, D. G. Whitten, *J. Phys. Chem.* **1982**, *86*, 3436-3439; g) G. B. Porter, R. H. Sparks, *J. Photochem.* **1980**, *13*, 123-131; h) B. Durham, J. V. Caspar, J. K. Nagle, T. J. Meyer, *J. Am. Chem. Soc.* **1982**, *104*, 4803-4810.

[8] a) W. R. McNamara, Z. Han, C.-J. Yin, W. W. Brennessel, P. L. Holland, R. Eisenberg, *Proc. Natl. Acad. Sci. U.S.A.* **2012**, *39*, 15594–15599; b) Y. Sun, J. Sun, J. R. Long, P. Yang, C. J. Chang, *Chem. Sci.* **2013**, *4*, 118-124; c) D. Streich, Y. Astuti, M. Orlandi, L. Schwartz, R. Lomoth, L. Hammarström, S. Ott, *Chem. Eur. J.* **2010**, *16*, 60-63.

[9] a) J. L. Dempsey, B. S. Brunschwig, J. R. Winkler, H. B. Gray, *Acc. Chem. Res.* **2009**, *42*, 1995-2004; b) M. L. Helm, M. P. Stewart, R. M. Bullock, M. R. DuBois, D. L. DuBois, *Science* **2011**, *333*, 863-866; c) H. I. Karunadasa, E. Montalvo, Y. Sun, M. Majda, J. R. Long, C. J. Chang, *Science* **2012**, *335*, 698-702; d) H. I. Karunadasa, C. J. Chang, J. R. Long, *Nature* **2010**, *464*, 1329-1333; e) Z. Han, F. Qiu, R. Eisenberg, P. L. Holland, T. D. Krauss, *Science* **2012**, *338*, 1321-1324.

[10] a) P. N. Curtin, L. L. Tinker, C. M. Burgess, E. D. Cline, S. Bernhard, *Inorg. Chem.* **2009**, *48*, 10498-10506; b) E. D. Cline, S. E. Adamson, S.

Bernhard, *Inorg. Chem.* **2008**, *47*, 10378-10388; c) L. L. Tinker, N. D. McDaniel, P. N. Curtin, C. K. Smith, M. J. Ireland, S. Bernhard, *Chem. Eur. J.* **2007**, *13*, 8726-8732; d) J. I. Goldsmith, W. R. Hudson, M. S. Lowry, T. H. Anderson, S. Bernhard, *J. Am. Chem. Soc.* **2005**, *127*, 7502-7510.

[11] a) M. Guttentag, A. Rodenberg, C. Bachmann, A. Senn, P. Hamm, R. Alberto, *Dalton Trans.* **2012**, *42*, 334-337; b) B. Probst, C. Kolano, P. Hamm, R. Alberto, *Inorg. Chem.* **2009**, *48*, 1836-1843.

[12] a) X. H. Wang, S. Goeb, Z. Q. Ji, N. A. Pogulaichenko, F. N. Castellano, *Inorg. Chem.* **2011**, *50*, 705-707; b) P. Du, K. Knowles, R. Eisenberg, *J. Am. Chem. Soc.* **2008**, *130*, 12576-12577.

[13] a) Z. Han, W. R. McNamara, M.-S. Eum, P. L. Holland, R. Eisenberg, *Angew. Chem. Int. Ed.* **2012**, *51*, 1667-1670; b) T. Lazarides, T. McCormick, P. Du, G. Luo, B. Lindley, R. Eisenberg, *J. Am. Chem. Soc.* **2009**, *131*, 9192-9194; c) J. Dong, M. Wang, P. Zhang, S. Yang, J. Liu, X. Li, L. Sun, *J. Phys. Chem. C* **2011**, *115*, 15089-15096.

[14] a) P. W. Du, J. Schneider, G. G. Luo, W. W. Brennessel, R. Eisenberg, *Inorg. Chem.* **2009**, *48*, 4952-4962; b) T. M. McCormick, Z. Han, D. J. Weinberg, W. W. Brennessel, P. L. Holland, R. Eisenberg, *Inorg. Chem.* **2011**, *50*, 10660-10666.

[15] W. R. McNamara, Z. J. Han, P. J. Alperin, W. W. Brennessel, P. L. Holland, R. Eisenberg, *J. Am. Chem. Soc.* **2011**, *133*, 15368-15371.

[16] a) F. d. r. Gloaguen, J. D. Lawrence, T. B. Rauchfuss, *J. Am. Chem. Soc.* **2001**, *123*, 9476-9477; b) M. J. Rose, H. B. Gray, J. R. Winkler, *J. Am. Chem. Soc.* **2012**, *134*, 8310-8313.

[17] Z. J. Han, W. R. McNamara, M. S. Eum, P. L. Holland, R. Eisenberg, *Angew. Chem. Int. Ed.* **2012**, *51*, 1667-1670.

[18] a) M. Nippe, R. S. Khnayzer, J. A. Panetier, D. Z. Zee, B. S. Olaiya, M. Head-Gordon, C. J. Chang, F. N. Castellano, J. R. Long, *Chem. Sci.* **2013**; b) Y. J. Sun, J. W. Sun, J. R. Long, P. D. Yang, C. J. Chang, *Chem. Sci.* **2013**, *4*, 118-124; c) M. Guttentag, A. Rodenberg, C. Bachmann, A. Senn, P. Hamm, R. Alberto, *Dalton Trans.* **2013**, *42*, 334-337; d) J. P. Bigi, T. E. Hanna, W. H. Harman, A. Chang, C. J. Chang, *Chem. Commun.* **2010**, *46*, 958-960.

[19] M. Elvington, J. Brown, S. M. Arachchige, K. J. Brewer, *J. Am. Chem. Soc.* **2007**, *129*, 10644-10645.

[20] N. V. Rees, O. V. Klymenko, R. G. Compton, M. Oyama, *J. Electroanal. Chem.* **2002**, *531*, 33-42.

[21] R. S. Khnayzer, C. E. McCusker, B. S. Olaiya, F. N. Castellano, *J. Am. Chem. Soc.* **2013**, *135*, 14068-14070.

[22] B. Probst, M. Guttentag, A. Rodenberg, P. Hamm, R. Alberto, *Inorg. Chem.* **2011**, *50*, 3404-3412.

[23] C. V. Krishnan, N. Sutin, *J. Am. Chem. Soc.* **1981**, *103*, 2141-2142.

[24] J. L. Dempsey, J. R. Winkler, H. B. Gray, *J. Am. Chem. Soc.* **2010**, *132*, 1060-1065.

[25] R. S. Khnayzer, V. S. Thoi, M. Nippe, A. E. King, J. W. Jurss, K. A. El Roz, J. R. Long, C. J. Chang, F. N. Castellano, *Energy Environ. Sci.* **2014**, *7*, 1477-1488.

[26] K. Kalyanasundaram, *Coord. Chem. Rev.* **1982**, *46*, 159-244.

[27] G. Accorsi, A. Listorti, K. Yoosaf, N. Armaroli, *Chem. Soc. Rev.* **2009**, *38*, 1690-1700.

[28] R. S. Khnayzer, L. B. Thompson, M. Zamkov, S. Ardo, G. J. Meyer, C. J. Murphy, F. N. Castellano, *J. Phys. Chem. C* **2012**, *116*, 1429-1438.

[29] a) V. Artero, M. Chavarot-Kerlidou, M. Fontecave, *Angew. Chem. Int. Ed.* **2011**, *50*, 7238-7266; b) P. Du, R. Eisenberg, *Energy Environ. Sci.* **2012**, *5*, 6012-6021.

[30] a) X. L. Hu, B. S. Brunschwig, J. C. Peters, *J. Am. Chem. Soc.* **2007**, *129*, 8988-8998; b) C. Baffert, V. Artero, M. Fontecave, *Inorg. Chem.* **2007**, *46*, 1817-1824; c) M. Razavet, V. Artero, M. Fontecave, *Inorg. Chem.* **2005**, *44*, 4786-4795.

[31] a) G. N. Schrauzer, *Inorg. Synth.* **1968**, *11*, 61-70; b) G. N. Schrauzer, *Acc. Chem. Res.* **1968**, *1*, 97-103.

[32] a) M. Nippe, R. S. Khnayzer, J. A. Panetier, D. Z. Zee, B. S. Olaiya, M. Head-Gordon, C. J. Chang, F. N. Castellano, J. R. Long, *Chem. Sci.* **2013**, *4*, 3934-3945; b) R. S. Khnayzer, D. R. Martin, C. L. Codding, F. N. Castellano, *Rev. Sci. Instrum.* **2015**, *86*, 034101.

[33] a) M. Ruthkosky, F. N. Castellano, G. J. Meyer, *Inorg. Chem.* **1996**, *35*, 6406-6412; b) T. E. Mallouk, J. S. Krueger, J. E. Mayer, C. M. G. Dymond, *Inorg. Chem.* **1989**, *28*, 3507-3510.

Entry for the Table of Contents

Layout 1:

FULL PAPER

Hydrogen is a desirable feedstock chemical for carbon-free energy technologies. In this work, we demonstrate that the bathophenanthroline ligand framework imparts greater stability onto ruthenium (II) photosensitizer then its bipyridyl congener while maintaining favourable kinetics and energetics for photocatalytic hydrogen evolution.

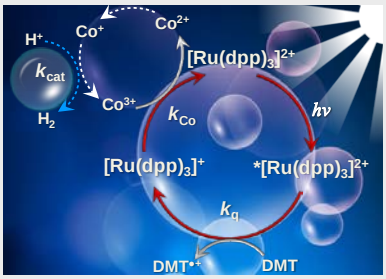

Rony S. Khnayzer, Babatunde S. Olaiya, Karim A. El Roz and Felix N. Castellano**

Page No. – Page No.

Homogeneous Photocatalytic H_2 Production using a Ru(II) Bathophenanthroline MLCT Photosensitizer